INFLUENCE OF MASTICATION ON THE MICROSTRUCTURE AND PHYSICAL PROPERTIES OF RUBBER

KOJI OKAMOTO,[1] MICHIHARU TOH,[2] XIAOBIN LIANG,[3] KEN NAKAJIMA[3,4,*]

[1]NIHON SPINDLE MANUFACTURING, 4-2-30, SHIOE AMAGASAKI, HYOGO 661-8510, JAPAN
[2]5123, OAZA-SASAGURI, SASAGURI, KASUYA, FUKUOKA 811-2405, JAPAN
[3]DEPARTMENT OF CHEMICAL SCIENCE AND ENGINEERING, TOKYO INSTITUTE OF TECHNOLOGY, 2-12-1 OOKAYAMA, MEGURO-KU, TOKYO 152-8550, JAPAN
[4]DEPARTMENT OF APPLIED PHYSICS, GRADUATE SCHOOL OF ENGINEERING, THE UNIVERSITY OF TOKYO, 7-3-1 HONGO, BUNKYO-KU, TOKYO 113-8656, JAPAN

RUBBER CHEMISTRY AND TECHNOLOGY, Vol. 94, No. 3, pp. 533–548 (2021)

ABSTRACT

The effects of the masticated state of isoprene rubber (IR) at the carbon black (CB) addition stage on subsequent mixing, microstructure, and physical properties in the case of a kneader with a characteristic large-diameter shaft are investigated by examining the mastication-time dependence. A sufficiently masticated IR shows a shorter black incorporation time, which results in an improved dispersion of CB and better physical properties. Observing the microstructure of a rubber compound using the atomic force microscope–based nanomechanical technique, poor CB dispersion is revealed for insufficient mastication. Specifically, large CB agglomerations surrounded by the interfacial rubber region with higher elastic modulus than that of a rubber matrix are formed. Such a large CB agglomeration, on the other hand, does not appear in rubber compounds with longer mastication times. The thickness of the interfacial region becomes shorter in these cases. These observations are further discussed by the concept of "rheological unit" introduced by Mooney et al. This study demonstrates that the microstructure of a rubber compound is highly heterogenous with rubber regions of different microscopic elastic moduli and that the microstructure has an influence on CB dispersion and the physical properties of rubber. [doi:10.5254/rct.21.79952]

INTRODUCTION

More than 100 years ago, rubber reinforcement with carbon black (CB) was discovered. Since the initial development of an open-mill mixer, an internal mixer with tangential/intermeshing rotors and a drop door/tilt chamber has been invented. The microstructure of CB in CB-reinforced rubbers formed by these mixers is responsible for their physical properties. To date, CB dispersion has been evaluated from the mixing time and power consumption using a Banbury mixer with a tangential rotor,[1–3] intermeshing mixer,[4,5] and both.[6,7] In addition, it has been studied by observing CB aggregates,[8–11] the effective filler volume fraction,[12,13] electric conductivity,[14,15] and T_2 of NMR relaxation.[16,17]

The CB dispersion has been modeled. For example, a typical process model of CB dispersion is as follows. In the first macroscopic step, raw rubber undergoes a large deformation, increasing its surface area. Raw rubber then relaxes and incorporates CB. In the second microscopic step, the raw rubber, which is finely subdivided, comes into contact with CB to disperse CB on the μm order. However, the second step has yet to be confirmed in practice.[18,19] In another model of the microstructure of CB-reinforced rubber, CB-reinforced rubber is divided into two phases: the agglomerate phase, which has plastic-like characteristics and includes CB, and the free polymer phase, which has rubbery characteristics without CB. This agglomerate phase is connected as a continuous region.[20]

CB is efficiently dispersed, reducing the time necessary to achieve a uniform dispersion in the following two cases: (1) when the state of raw rubber immediately before the addition of CB has a large elongation at break and shows a behavior that allows plastic deformation,[21] and (2) when the

*Corresponding author. Email: knakaji@polymer.titech.ac.jp

TABLE I
RECIPE OF CB-REINFORCED COMPOUND IN IR

Ingredient	Without Sulfur, phr	With Sulfur, phr
Isoprene rubber (IR2200)	100	100
Carbon black (N550)	40	40
ZnO	3	3
Stearic acid	1	1
Sulfur		2
Accelerator CBS		1

large surface area of raw rubber is in contact with CB by increasing mastication time.[22] However, the effects of raw rubber mastication on subsequent mixing, microstructure, and rubber properties have yet to be reported. In addition, previous studies on mastication used a drop-door–type Banbury mixer. An internal mixer (kneader) with the tangential rotor, tilt chamber, and pressure lid has not been reported.

This article investigates the influence of mastication time in mixing isoprene rubber (IR) and CB by a kneader. That is, the effects of the mastication state before the addition of CB on the subsequent mixing, microstructure, and physical properties are elucidated. The microstructure of rubber is obtained from an analytical technique called atomic force microscopy (AFM)–based nanomechanical mapping[23–25] developed by Nakajima et al. The technique measures micro-elastic moduli and the adhesive force of a rubber surface with at a nm resolution. It allows the state of the interface region between CB and the rubber region in CB-reinforced rubber to be understood.

EXPERIMENTAL

MASTICATION OF IR WITH A KNEADER

Table I shows the recipe of CB-reinforced rubber in IR. Rubber mixing was performed using a kneader with a characteristic large-diameter shaft (chamber volume 2.5 L, Nihon Spindle Manufacturing, Amagasaki, Japan) shown in Figure 1. The process involved the following steps. First, raw rubber was masticated at five durations of 0.5, 1, 3, 5, or 10 min. The surface temperature of the chamber at the start was between 45 to 50 °C. Next, all ingredients were added, except for the raw rubber specimen. For the first 30 s, it was mixed without pressure-lid pressure. The pressure lid was then gradually lowered for 30 s until reaching a pressure of 0.5 MPa. Namely, the mixing under pressure was started after 1 min. The specimens were mixed until the maximum electric power was reached. the pressure lid was then moved up and down once and further mixed for an additional 3 min. The mixing occurred at a constant rotor speed of 30 rpm and a constant pressure-lid pressure of 0.5 MPa. This method provided samples of masticated raw rubber formed in the first mastication and samples of rubber compound that were mixed to the end.

SHEET MOLDING OF MASTICATED IR AND RUBBER COMPOUND WITHOUT SULFUR

At first, masticated IR2200 (Zeon, Tokyo, Japan) and IR compound without sulfur were sheeted in one pass with an 8-inch open mill (Kansai Roll, Osaka, Japan) at 60 °C. Next, each sample was pressed at 100 °C for 5 min and subsequently cooled to room temperature. This mold realized approximately 2 mm thick unvulcanized rubber sheets.

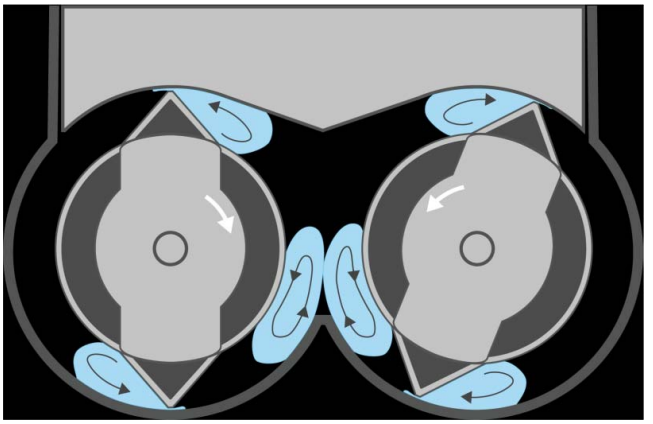

FIG. 1. — Kneader with a tangential rotor.

VULCANIZED RUBBER SHEET MOLDING OF RUBBER COMPOUND WITH SULFUR

The IR compound with sulfur was sheeted in one pass with an 8 inch open mill at 60 °C. Then, a 2 mm thick vulcanized rubber sheet was obtained under the conditions of 150 °C for 20 min using each rubber compound with sulfur.

MEASUREMENT METHOD OF THE PHYSICAL PROPERTIES OF RUBBER

The molecular weight, Mooney viscosity, and viscoelastic properties were measured using Waters2695 (Waters, Milford, MA, USA), SMV-202 (Shimadzu, Kyoto, Japan), and AR2000ex (TA Instruments, New Castle, DE, USA) with the sheet of masticated IR2200 and the sheet of IR compound without sulfur. Table II shows the measurement conditions. Tensile properties were measured according to ISO 37:2011 with a dumbbell No. 3 shape at a tensile speed of 500 mm/min using AG-1kNXDplus (Shimadzu). The De Mattia fatigue was measured according to ISO 132:2011, and DIN abrasion was measured according to ISO 4649:2002.

MEASUREMENT OF MICRO-ELASTIC MODULI OF REINFORCED RUBBER

The micro-elastic moduli of rubber specimens were measured by AFM-based nanomechanical measurement. After making a rubber surface to be measured with a microtome at –120 °C, the micro-elastic moduli of rubber specimens were measured by ForceVolume measurements using NanoScope V (Bruker, Billerica, MA, USA) with the cantilever, OMCL-TR800PSA (Olympus, Tokyo, Japan). The spring constant of the cantilever was measured to be $k = 0.93$ N/m. The radius of the curvature was also measured with the blind reconstruction method, and it was $R = 11$ nm. Micro-

TABLE II
CONDITIONS FOR VISCOELASTICITY MEASUREMENT OF MASTICATED IR AND A COMPOUND WITHOUT SULFUR

	Masticated IR	CB reinforced compound
Temperature, °C	25–105	80
Shear strain, %	0.50	0.04–6
Frequency, Hz	1	1

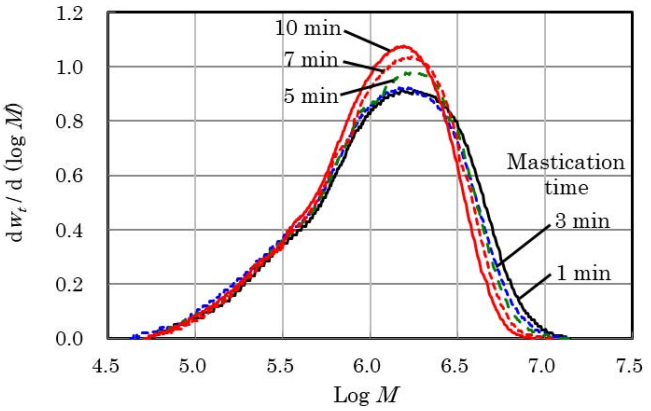

FIG. 2. — Molecular weight distributions of masticated IR.

elastic moduli obtained by this method were calculated based on Johnson-Kendall-Robert (JKR) contact mechanics.[26] Here, they are referred to as the JKR elastic moduli.

RESULTS AND DISCUSSION

CHANGE OF STATE OF MASTICATED IR BY PROLONGING THE MASTICATION TIME

Figure 2 shows the relationship between the mastication time of masticated IR by the kneader and the molecular weight distribution. The high-molecular-weight component decreases with mastication time. Figure 3 shows the temperature dependence of the viscoelastic properties for masticated IR at different mastication times. As the mastication time is prolonged, the storage elastic modulus G' decreases, whereas the loss elastic modulus G'' and the loss tangent increase. In addition, the same tendency is observed upon increasing the temperature. Figure 4 shows the relationship between the temperature at the end of masticated IR and mastication time. Because the temperature of the masticated IR increases with the mastication time, the decrease in G' as well as the increase of G'' and the loss tangent become more obvious as the mastication time increases. Based on previous reports[21] that CB is efficiently dispersed when masticated raw rubber shows a plastic nature, the prolongation of mastication time tends to improve the dispersion of CB.

EFFECT ON RUBBER MIXING

Figure 5 shows a rubber mixing chart of the kneader with a masticating time of (a) 0.5, (b) 1, (c) 3, (d) 5, and (e) 10 min for the IR compound without sulfur. Figure 6a shows the relationship between the mastication time and black incorporation time (BIT) during rubber mixing. BIT is the time from the CB addition to the maximum electric power in the mixing chart, which is an indicator of the speed to incorporate CB.[27] BIT is shortened greatly to the case of 3 min mastication and then gradually shortened after that. Thus, the viscoelastic changes in masticated raw rubber affect the reduction of BIT in rubber mixing. Figure 6b shows the relationship between the mastication time and the total rubber mixing time. In this IR recipe, the total rubber mixing time with respect to the mastication time has a minimum value, which is obtained by mastication of 1 to 3 min. In short, prolonging the mastication shortens BIT in IR compounding, and the choice of moderate mastication time in rubber mixing is an effective means of shortening the total mixing time of IR compounds.

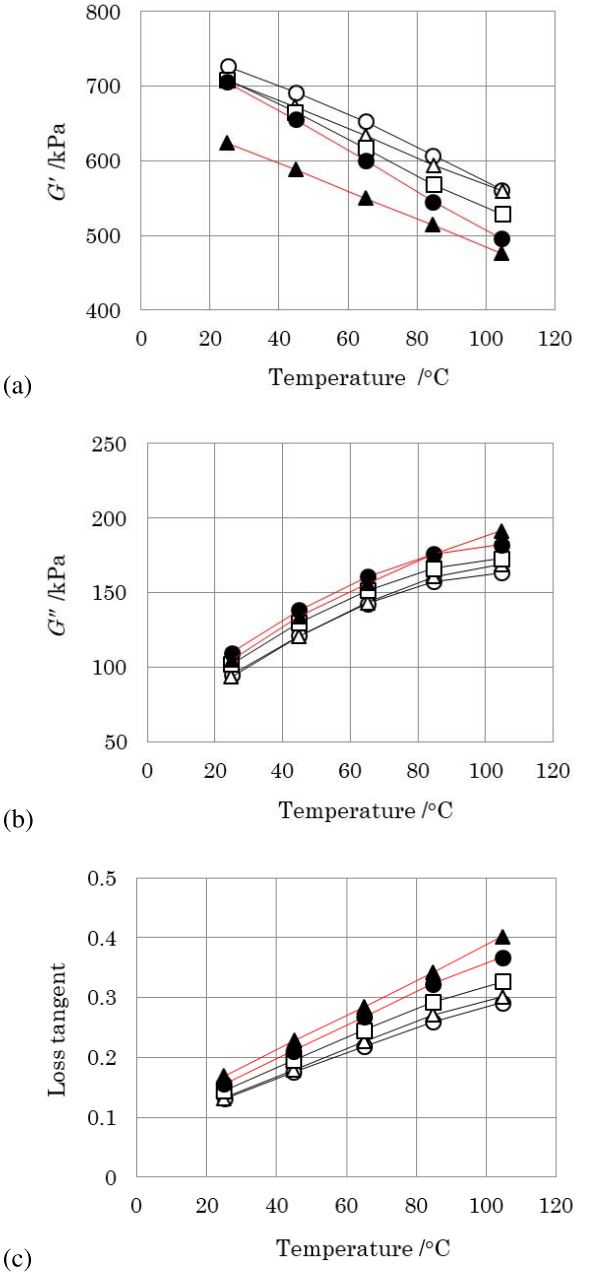

FIG. 3. — Temperature dependence of the viscoelastic properties for masticated IR at different mastication times. (a) G', (b) G'', and (c) loss tangent.

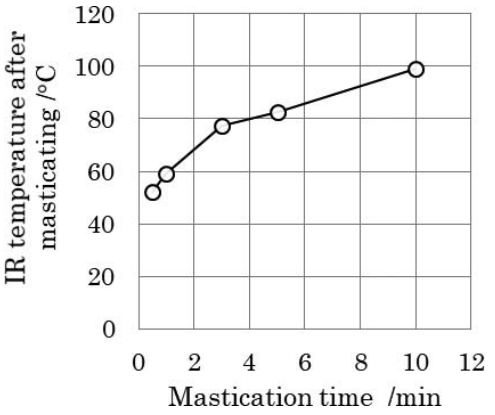

FIG. 4. — Relationship between the temperature of masticated IR and mastication time.

EFFECT ON THE PROPERTY OF RUBBER

Figure 7 shows the relationship between the mastication time of IR and G' (0.1%)/G' (4%) ratio in unvulcanized rubber. From the consideration of the so-called Payne effect,[28] the prolongation of mastication time decreases the G' (0.1%)/G' (4%) ratio and improves the dispersion of CB despite the shortened BIT. Similar to the trend seen in Figure 6a, the dispersion of CB improves greatly by the 3 min mastication followed by gradual improvement after that.

Figure 8 shows the relationship between the mastication time and the tensile properties of IR compounds with sulfur. The tensile strength and elongation at break shown in Figure 8a and b tend to decrease a little as the mastication time is prolonged, which might be attributed to the decrease in the high-molecular-weight component of IR. On the other hand, the modulus increases with the mastication time, as shown in Figure 8c, which is an effect of improving CB dispersion by increasing mastication. Next, Figure 9a shows the relationship between the mastication time and the crack length of the De Mattia fatigue. As the mastication time is prolonged, the crack length progression is greatly suppressed by 3 min and becomes almost constant after that. Figure 9b shows the relationship between the mastication time and the wear index of DIN abrasion. Similar to Figure 9a, the wear index is increased at the beginning and becomes nearly constant after 5 min. The difference in the masticated IR state manifests as an improvement in CB dispersion, which contributes to the improved fatigue property and wear resistance.

EFFECT ON THE MICROSTRUCTURE OF VULCANIZED RUBBER

Figure 10 shows the JKR elastic modulus mappings, adhesive force mappings, and transmission electron microscopy (TEM) images for the IR compound with sulfur. The AFM mappings were obtained by AFM with a two-dimensional scan area of 3.0 μm. In the JKR elastic modulus mappings, the green and blue areas denote high and low JKR elastic moduli, respectively. White areas are CB. In the adhesion force mapping images, the dark red areas are mostly CB with a low adhesion force, whereas the light red areas are rubber regions. Large CB agglomerations surrounded by rubber regions with high JKR elastic moduli are seen for the cases of 0.5 and 1 min mastication, but these agglomerations disappear for mastication of $\geq$3 min. Similarly, the TEM image shows CB agglomerations only at 0.5 min of mastication. They are not observed at longer mastication times. Because we cannot quantitatively analyze the modulus of the rubber region around CB in the TEM images, we consider the microstructure and moduli of rubber from the JKR elastic modulus images and adhesion force images obtained by AFM. Figure 11a shows the AFM

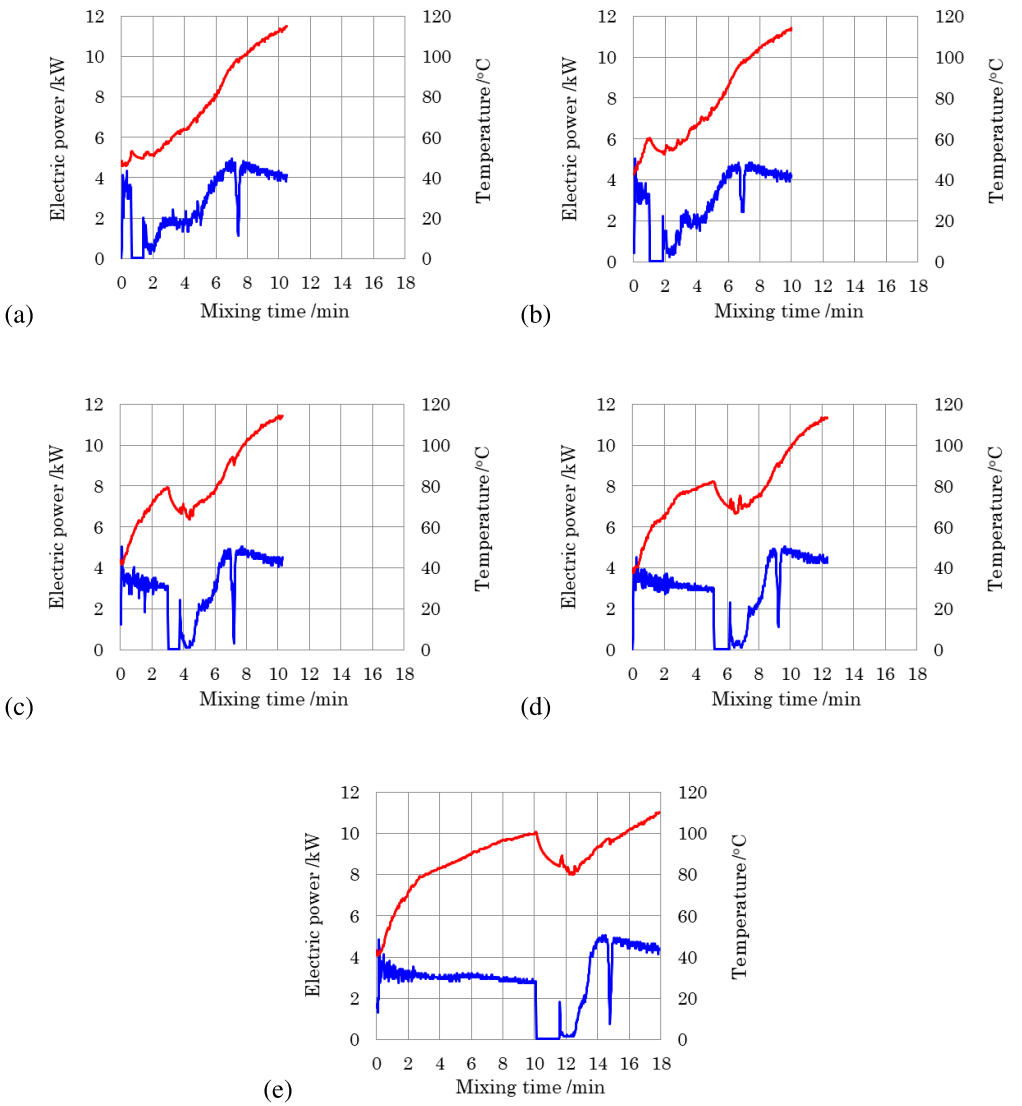

FIG. 5. — Mixing chart of the kneader as a function of mastication time. Mastication time: (a) 0.5 min, (b) 1 min, (c) 3 min, (d) 5 min, (e) 10 min.

topographic map for the 3 min mastication. Its histogram is also depicted in Figure 11b. The standard deviation over 3.0 μm × 3.0 μm was about 26 nm and became 15 nm if protrusive CB particle regions were excluded, which ensured the flatness of the rubber surface was reasonably suitable for AFM-based nanomechanical measurement.

Figure 12 shows four-valued mapping images of the JKR elastic modulus mapping images. These images consist of four regions: three rubber regions classified by the JKR elastic moduli and one region of the CB area.[29] The method for drawing four-valued mapping images is explained using the case of a 5 min mastication as an example. Figure 13a shows the histogram of an adhesive force mapping image, in which four Gaussian functions are used to fit the histogram curve. The lowest adhesive force side is the peak of CB, and the rest is attributed to the rubber regions. The

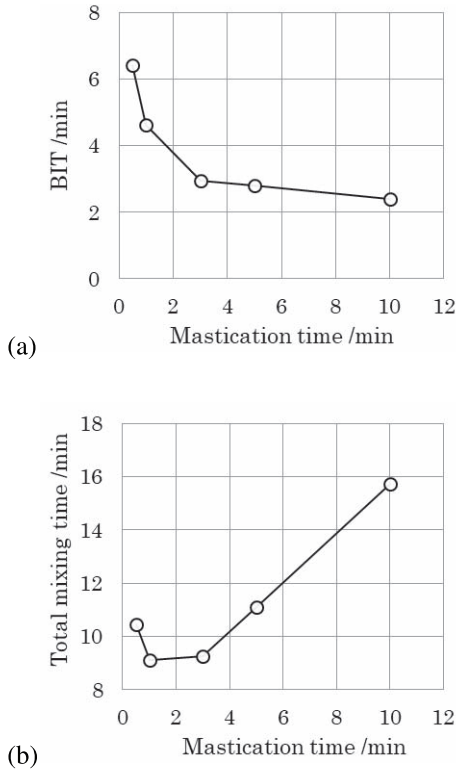

FIG. 6. — Relationship between (a) BIT, (b) the total mixing time of the IR compound, and mastication time.

fitting curve in the rubber region is composed of three curves with peak values of 2.6 nN, 3.6 nN, and 4.3 nN. Here, the fraction of CB is 0.122, which is a little bit lower but comparable with the volume fraction of CB estimated from the recipe (0.17). The fraction value obtained by AFM fluctuated depending on the imaging locations. This fluctuation can be used to measure the heterogeneity due to mixing condition, which will be our future study. By performing similar procedures, the fractions of CB were also determined to be 0.190, 0.138, 0.130, and 0.122 for 0.5, 1, 3, and 10 min for other mastication time, respectively.

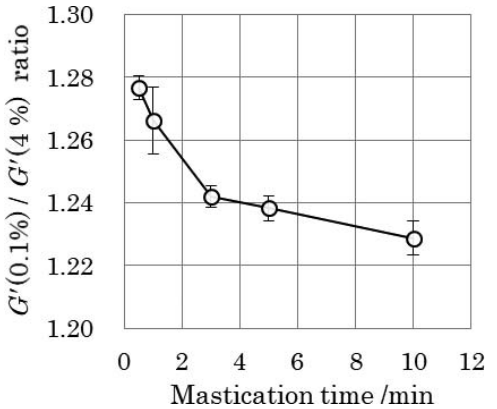

FIG. 7. — Relationship between the G' (0.1%)/G' (4%) ratio at 80 °C of IR and mastication time.

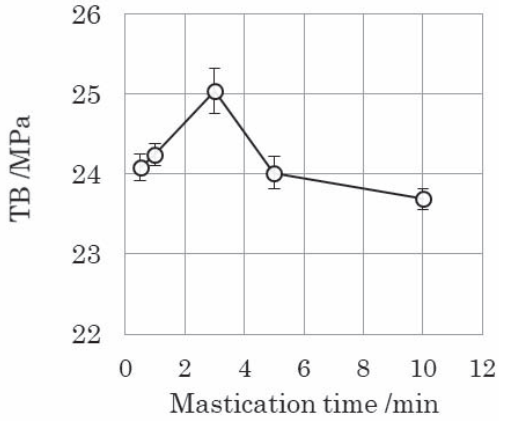

(a)

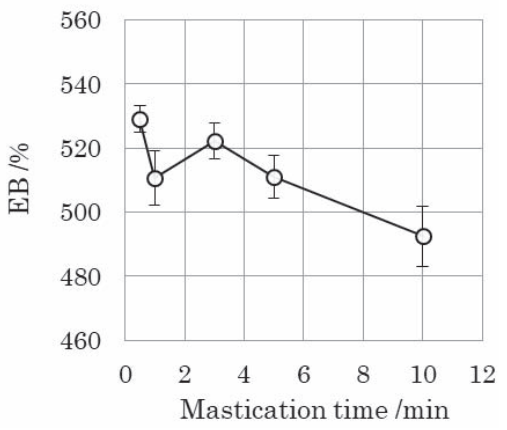

(b)

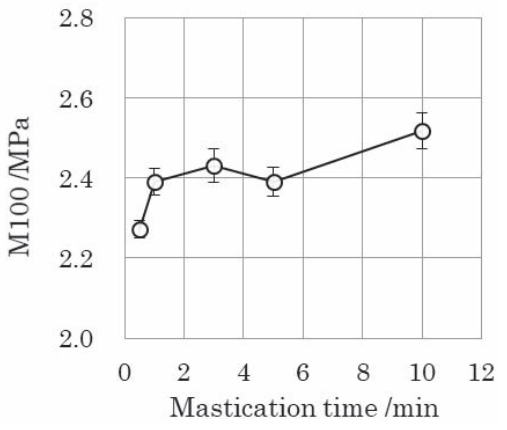

(c)

FIG. 8. — Relationship between the tensile properties and mastication time. (a) Tensile strength (TB), (b) elongation at break (EB), and (c) modulus (M100).

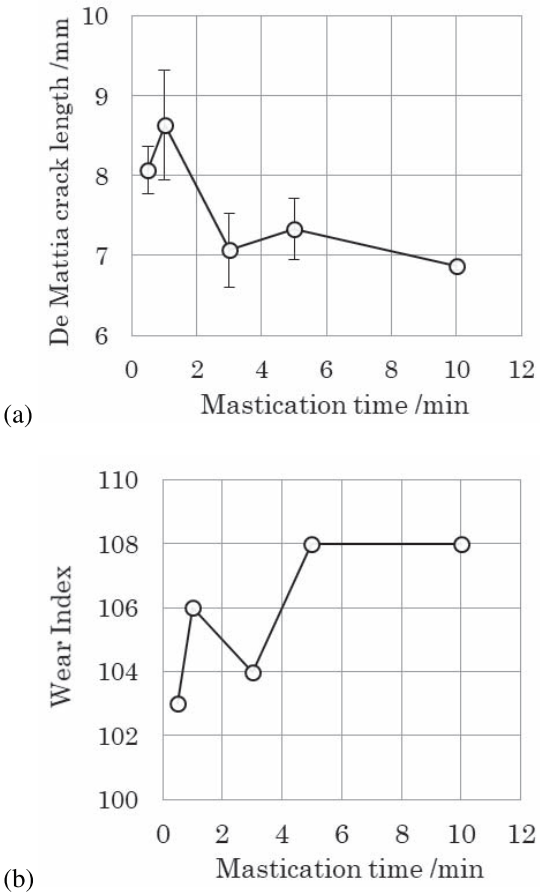

FIG. 9. — Relationship between (a) the crack length on the De Mattia fatigue measurement, (b) the wear index in DIN abrasion measurement, and mastication time.

Figure 13b shows a histogram of the JKR elastic moduli of the rubber region only, which does not contain the CB region with a volume fraction of 0.122 eliminated in the above procedure. The rubber region is fitted with three components, and these regions are called the high JKR elastic modulus region, the middle JKR elastic modulus region, and the low JKR elastic modulus region. In the four-valued mapping image, CB with a volume fraction of 0.122 is white, and the other rubber regions with a volume fraction of 0.878 are divided into three at the two intersections of the three fitting curves of the JKR elastic moduli. In Figure 12, blue, red, and black denote the low, middle, and high JKR elastic modulus regions, respectively. The high JKR elastic moduli region always exists around CB with a thickness less than 20 nm, including bound rubber. A similar value has been reported in the literature.[25,30]

Large CB agglomerations surrounded by the middle JKR elastic modulus regions as well as the large low JKR elastic modulus regions are observed in the case of 0.5 min mastication (Figure 12a). Moreover, similar large CB agglomerations appear at 1 min of mastication, although they look smaller than that at 0.5 min. When the IR is masticated for 3 min or longer, the agglomeration of CB disappears. This micro-structural change, in which 3 min mastication is regarded as a borderline, exhibits the same trend and therefore should have high relevance with the $G'(0.1\%)/G'(4\%)$ ratio,

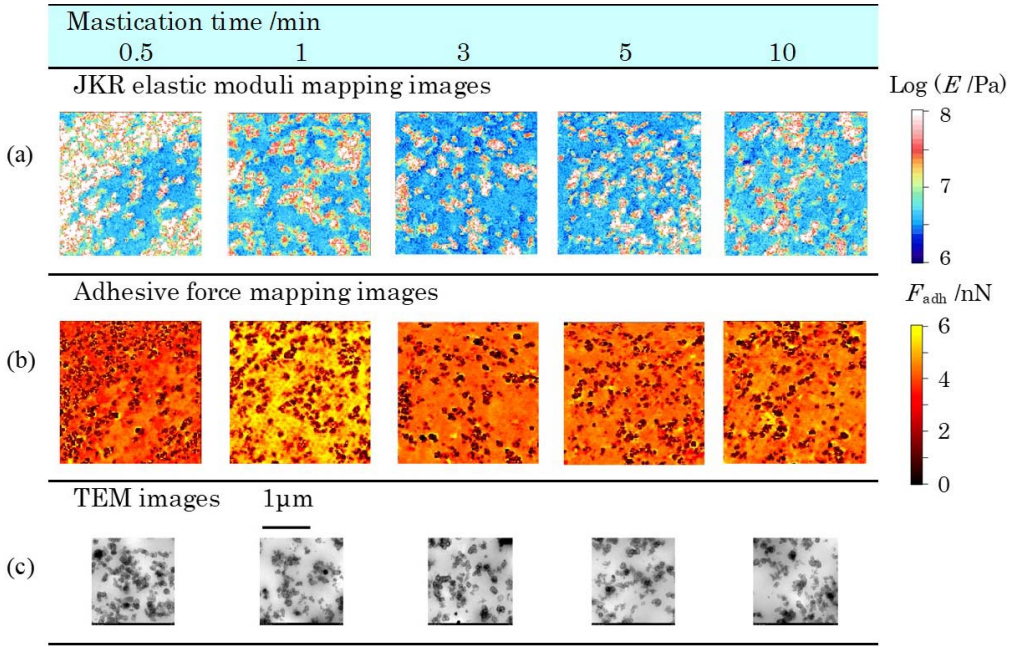

FIG. 10. — (a) JKR elastic moduli mappings, (b) adhesive force mappings by AFM, and (c) TEM images. The scan size of AFM is 3.0 μm and that of TEM is 2.0 μm.

the De Mattia fatigue, and the wear index of DIN abrasion. Hence, it is concluded that the mastication time affects the state of masticated IR, which in turn affects the state of the rubber region around the CB (i.e., the interfacial region) in the rubber microstructure. In addition, it is also concluded that the rubber region has a heterogeneous structure composed of different JKR elastic modulus regions, which is evidenced only by this AFM-based technique.

Figure 14a shows the relationship between the mastication time and the fraction of each of the three components in the rubber region after excluding CB regions, namely, the fractions of different rubber stiffness components relative to just the total rubber fraction of the compound, not the total

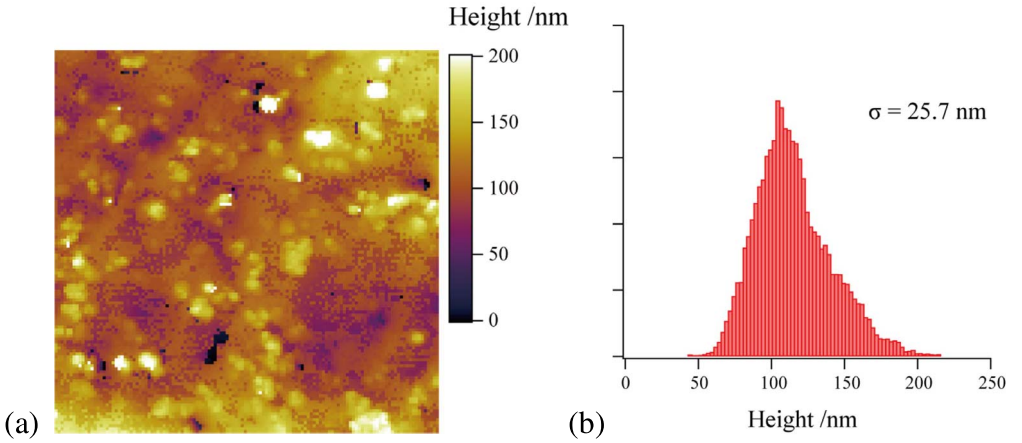

FIG. 11. — (a) Topographic image (3.0 μm) of mastication time of 3 min and (b) its histogram.

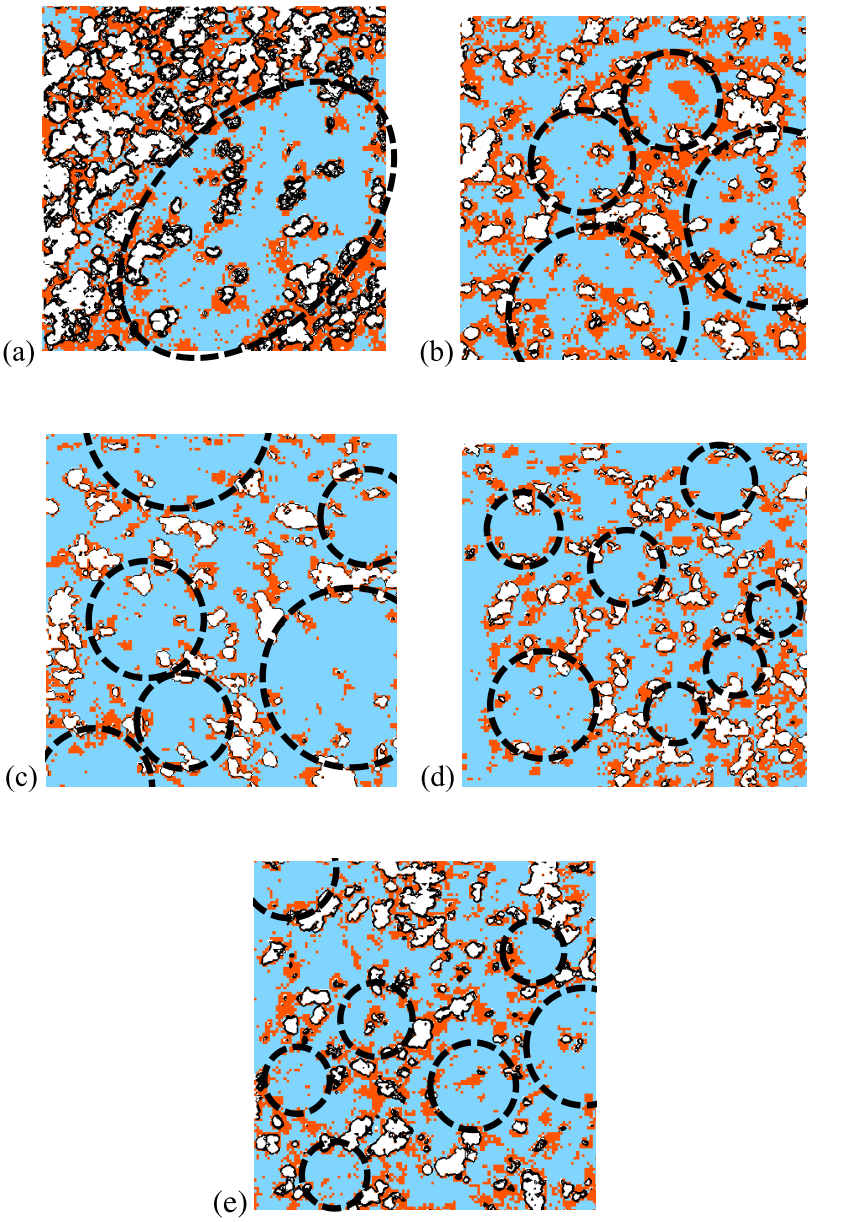

FIG. 12. — Four-valued mapping images of the JKR elastic moduli. Mastication time: (a) 0.5 min, (b) 1 min, (c) 3 min, (d) 5 min, and (e) 10 min. The supposed rheological units discussed in the "Effect of the State of Masticated IR on Rubber Mixing, Microstructure, and Physical Properties" are depicted as ellipses drawn with dashed line.

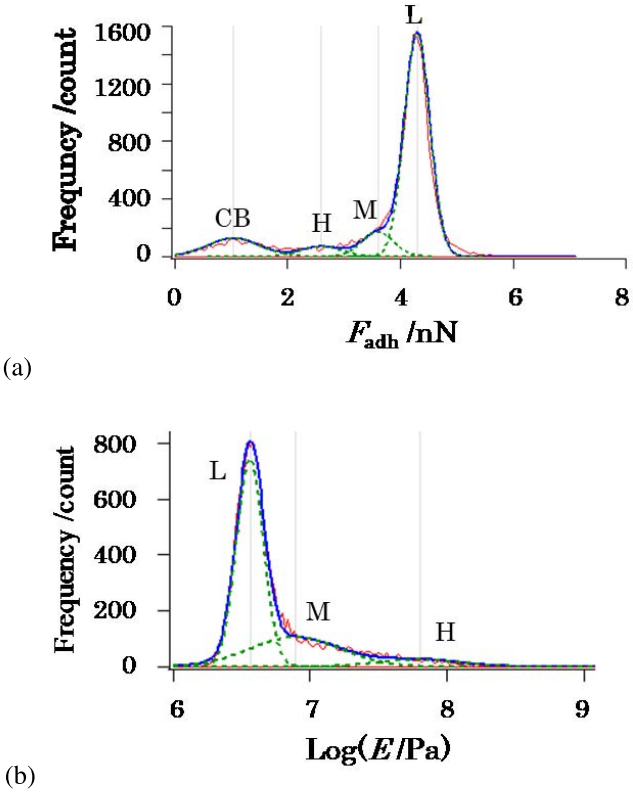

FIG. 13. — Histograms of (a) the adhesive force mapping image and (b) the JKR elastic moduli mapping image without a CB area for 5 min of mastication.

volume of compound. The low JKR elastic modulus region increases with time before 3 min of mastication but becomes nearly constant after 3 min of mastication. Oppositely, the middle and high JKR elastic modulus regions decrease at the beginning and become constant. Figure 14b shows the relationship between the mastication time and the peak JKR elastic moduli for low and middle JKR elastic modulus regions. The peak values are estimated by the curve fitting, as shown in Figure 13b. The peak value for the middle JKR elastic region decreases a little with time before 3 min of mastication but becomes nearly constant after that. This initial decrease would be attributed to the decrease in the high-molecular-weight component. On the other hand, the peak value for the low JKR elastic region is less affected by mastication time. These results indicate that the effect of mastication, especially before the 3 min mastication time, namely, the change in the state of masticated IR, results in the change kin the rubber region around CB (i.e., the interfacial region). The effect contributes less to the values of the middle and low JKR modulus regions.

Before going to the last discussion section, we report the condition of the elastic band immediately after discharging masticated IR and winding it around an 8 inch open mill. The elastic band has holes with a mastication time of less than 1 min, but these holes disappear after 3 min. Moreover, the skin of the elastic band becomes smoother for a longer mastication time. White[31] reported that mixing by an internal mixer was appropriately conducted when an elastic band nicely wound around a rotor as well as in the case of an open mill. Thus, the changes in appearance of the macroscopic elastic band before and after a mastication time of 3 min also has a deep relationship with the microscopic rubber states.

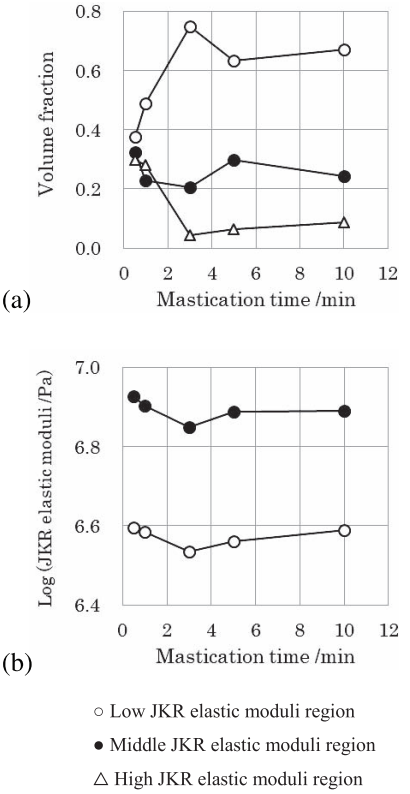

FIG. 14. — Relationship between mastication time and (a) the fractions of JKR elastic moduli in three rubber regions and (b) the peak values of JKR elastic moduli in two rubber regions.

EFFECT OF THE STATE OF MASTICATED IR ON RUBBER MIXING, MICROSTRUCTURE, AND PHYSICAL PROPERTIES

Here, the above-mentioned influence is considered from a different viewpoint. Mooney et al. experimentally demonstrated that when raw rubber is continuously sheared and broken over time, it subdivides into fine particles with a μm-order size.[32,33] These fine particles cannot be further divided because of the entanglement effect. Pale Crepe, SBR, NBR, and IIR have also been reported to subdivide into fine particles. This is the idea behind the second step, called the micro-step, in the model of CB dispersion progress mentioned above.[18] Mooney et al. called these subdivided raw rubber particles "rheological units."

The results of the above-mentioned IR masticating, rubber mixing, rubber microstructure, and CB dispersion are considered using the rheological unit concept. As the mastication time increases, the loss tangent of IR increases (Figure 3c), IR is subdivided, and the specific surface area increases. In this way, a sufficiently masticated IR turns into an assembly of rheological units with almost the same size in the order of sub-μm. After the addition of CB, these μm-order rheological units that have a large contact area easily incorporate CB agglomerations (shortened BIT in Figure 6a). Consequently, the CB agglomeration is uniformly dispersed, and the rubber microstructure is formed in which there exists neither large CB agglomeration nor a large rubber region, as shown in Figure 12c–e. Supposed rheological units are depicted in Figure 12 as ellipses drawn with a dashed line. On the other hand, if the mastication of IR is insufficient, plasticization, subdivision of IR, incorporation of CB, and dispersion of CB proceed simultaneously. In addition, CB is incorporated

in the IR state with a small loss tangent (Figure 3c), and large rheological units, which are not sufficiently subdivided, come into contact with CB. For this reason, BIT becomes longer, making it more difficult to disperse CB on the microscale. Thus, the large CB agglomeration and the large rubber region remain as evidenced in Figure 12a,b. In summary, it is speculated that the dispersion of CB is largely affected by the size of rheological units during the mastication process.

Next, we compare the microstructure of IR compounds obtained this time with that for the previously reported model of CB-reinforced rubber.[20] The model structure is divided into two phases: the agglomerate phase, which has plastic-like characteristics and includes CB, and the free polymer phase, which has rubbery characteristics without CB. Furthermore, the agglomerate phase is connected as a continuous region. This is similar to the four-valued mapping image for the case of 0.5 min mastication in Figure 12a, in which large CB agglomerations are surrounded by the middle JKR elastic moduli region. Because these large CB agglomerations disappear after a mastication of 3 min, the previous model is valid only when the mastication time is short. They become dissimilar to each other when sufficiently masticated with a prolonged mastication time. Further examination is necessary.

CONCLUSION

We investigated the effect of the mastication state of IR at the CB addition stage on subsequent mixing, microstructure, and physical properties in the case of a kneader with a characteristic large-diameter shaft. We found that high-molecular-weight rubber components and G' decrease and that G'' and the loss tangent increase concomitantly with mastication time for masticated IR. This change in the masticated IR state shortens the BIT and improves CB dispersion. It also affects the De Mattia fatigue properties and DIN wear properties of rubber. The AFM nanomechanical mapping technique revealed that CB dispersion is poor in the case of insufficient mastication. Specifically, large CB agglomerations surrounded by the interfacial rubber region (middle JKR elastic moduli region) between CB aggregates and the rubber region (low JKR elastic moduli region) are formed. On the other hand, when the CB dispersion is good and the physical properties are satisfactory, large agglomerations are not observed, and the interfacial region becomes thinner. These observations can be expressed by the concept of "rheological unit" introduced by Mooney et al. When the mastication time is insufficient and the subdivision of IR raw rubber is incomplete, the size of the rheological unit remains large and its size distribution is wide, resulting in the formation of large CB agglomerations. Thus, it becomes hard for CB to disperse further. In contrast, when the rheological units become smaller because of sufficient mastication, these rheological units contact with CB efficiently, resulting in the smoother incorporation and the dispersion of CB agglomerates. As a result, CB is well dispersed in the IR matrix. This study demonstrated that the microstructure of the rubber compound is highly heterogenous with rubber regions with different microscopic elastic moduli and that the microstructure has an influence on CB dispersion and the physical properties of rubber, which is clearly elucidated by the AFM-based nanomechanical mapping technique.

REFERENCES

[1]P. C. Ebell and D. A. Hermsley, RUBBER CHEM. TECHNOL. **54**, 698 (1981).

[2]W. M. Hess, R. A. Swor, and E. J. Micek, RUBBER CHEM. TECHNOL. **57**, 959 (1984).

[3]A. Y. Coran and J. B. Donnet, RUBBER CHEM. TECHNOL. **65**, 998 (1992).

[4]J. Clarke and P. K. Freakley, RUBBER CHEM. TECHNOL. **67**, 700 (1994).

[5]J. Narongthong, P. Sae-Oui, and C. Sirisinha, RUBBER CHEM. TECHNOL. **91**, 521 (2018).

[6]W. M. Wiedmann and H. M. Schmid, RUBBER CHEM. TECHNOL. **55**, 363 (1982).

[7]C. Koolhiran and J. L. White, *J. Appl. Polym. Sci*. **78**, 1551 (2000).
[8]B. B. Boonstra and A. I. Medalia, RUBBER CHEM. TECHNOL. **36**, 115 (1963).
[9]E. S. Dizon and L. A. Papazian, RUBBER CHEM. TECHNOL. **50**, 765 (1977).
[10]S. Shiga and M. Furuta, RUBBER CHEM. TECHNOL. **58**, 1 (1985).
[11]S. P. Rwei, I. Manas-Zloczower, and D. L. Feke, *Polym. Eng. Sci*. **30**, 701 (1990).
[12]P. K. Freakley and C. Sirsinha, *J. Appl. Polym. Sci*. **65**, 305 (1998).
[13]C. Sirsinha and W. Sittichokchuchai, *J. Appl. Polym. Sci*. **76**, 1542 (2000).
[14]B. B. Boonstra, RUBBER CHEM. TECHNOL. **50**, 194 (1977).
[15]H. H. Le, S. Ilisch, B. Jakob, and H. J. Radusch, RUBBER CHEM. TECHNOL. **77**, 147 (2004).
[16]T. Nishi, *J. Polym. Sci., Polym. Phys. Ed*. **12**, 685 (1974).
[17]H. Serizawa, M. Ito, T. Kanamoto, K. Tanaka, and A. Nomura, *Polym. J*. **14**, 149 (1982).
[18]N. Nakajima, RUBBER CHEM. TECHNOL. **53**, 1088 (1980).
[19]N. Nakajima and E. R. Harrell, RUBBER CHEM. TECHNOL. **57**, 153 (1984).
[20]A. Ahagon, RUBBER CHEM. TECHNOL. **71**, 975 (1998).
[21]N. Tokita and I. Pliskin, RUBBER CHEM. TECHNOL. **46**, 1166 (1973).
[22]A. Morikawa, K. Min, and J. L. White, *Adv. Polym. Technol*. **8**, 383 (1988).
[23]K. Nakajima, M. Ito, D. Wang, H. Liu, H. K. Nguyen, X. Liang, A. Kumagai, and S. Fujinami, *Microscopy* **63**,193 (2014).
[24]D. Wang, X. Liang, T. P. Russell, and K. Nakajima, *Macromolecules* **47**, 3761 (2014).
[25]K. Nakajima, M. Ito, H. K. Nguyen, and X. Liang, RUBBER CHEM. TECHNOL. **90**, 272 (2017).
[26]K. L. Johnson, K. Kendall, and A. D. Roberts, *Proc. R. Soc. Lond. A* **324**, 301 (1971).
[27]K. C. Beach, L. F. Comper, and V. E. Lowery, *Rubber Age* **85**, 253 (1959).
[28]A. R. Payne, *J. Appl. Polymer. Sci*. **9**, 2273 (1965).
[29]K. Okamoto, M. Toh, X. Liang, and K. Nakajima, "Influence of Mastication on Microstructure and Physical Properties of Rubber," International Rubber Conference, London, September 4, 2019.
[30]H. K. Nguyen, X. Liang, M. Ito, and K. Nakajima, *Macromolecules*, **51**, 6085 (2018).
[31]J. L. White, RUBBER CHEM. TECHNOL. **50**, 163 (1977).
[32]M. Mooney and W. E. Wolstenholme, *J. Appl. Phys*. **25**, 1098 (1954).
[33]M. Mooney and W. E. Wolstenholme, RUBBER CHEM. TECHNOL. **28**, 488 (1955).

[*Received May 2020, Revised March 2021*]